Protection of DNase in the shell of a pH-responsive, antibiotic-loaded micelle for biofilm targeting, dispersal and eradication

Tian, Shuang; Su, Linzhu; An, Yingli; van der Mei, Henny C.; Ren, Yijin; Busscher, Henk J.; Shi, Linqi

Published in:
Chemical Engineering Journal

DOI:
10.1016/j.cej.2022.139619

Publication date:
2023

Chemical Engineering Journal 452 (2023) 139619

Contents lists available at ScienceDirect

Chemical Engineering Journal

journal homepage: www.elsevier.com/locate/cej

Protection of DNase in the shell of a pH-responsive, antibiotic-loaded micelle for biofilm targeting, dispersal and eradication

Shuang Tian [a,b], Linzhu Su [a,b], Yingli An [a], Henny C. van der Mei [b,*], Yijin Ren [c], Henk J. Busscher [b,*], Linqi Shi [a,*]

[a] State Key Laboratory of Medicinal Chemical Biology, Key Laboratory of Functional Polymer Materials of Ministry of Education, and Institute of Polymer Chemistry, College of Chemistry, Nankai University, Tianjin 300071, PR China
[b] University of Groningen and University Medical Center Groningen, Department of Biomedical Engineering, Antonius Deusinglaan 1, 9713 AV Groningen, Netherlands
[c] University of Groningen and University Medical Center Groningen, Department of Orthodontics, Hanzeplein 1, 9700 RB Groningen, Netherlands

ARTICLE INFO

Keywords:
DNase I
Nanocarriers
Self-targeting
Biofilm
eDNA
Infection
Pneumonia

ABSTRACT

DNase can break down the extracellular matrix that keeps infectious bacterial biofilm together through cleavage of eDNA. Herewith, biofilm bacteria can become dispersed to assist antibiotic eradication but this has hitherto remained an *in vitro* possibility. *In vivo* DNase is rapidly broken down in blood, impeding blood-injection of DNase combined with antibiotics to cure bacterial infections. Herein, we report the synthesis of pH-responsive, self-targeting micelles self-assembled from a solution of poly(ethylene glycol)-*block*-poly(ε-caprolactone) (PEG-*b*-PCL) and poly(ε-caprolactone)-*block*-poly(amino ester) (PCL-*b*-PAE) with DNase conjugated to PAE-blocks. At physiological pH, this conjugation protected DNase inside the micellar shell, while PEG prevented adsorption of blood-borne proteins to the micelles. PAE became positively-charged below pH 6.4 facilitating self-targeting to an infectious biofilm. Simultaneously, PAE became hydrophilic and stretched to expose DNase upon accumulation in an infectious *S. aureus* biofilm where it degraded the biofilm matrix. PEG/PAE-DNase micelles internally core-loaded with ciprofloxacin significantly better eradicated murine pneumonia after blood-injection than ciprofloxacin-loaded PEG/PAE micelles without conjugated DNase or ciprofloxacin free in solution. Considering that DNase is clinically approved for use in cystic fibrosis patients, this paves the way for clinical translation of ciprofloxacin-loaded, PEG/PAE-DNase micelles for the treatment of pneumonia and other infections that can be reached through self-targeting after blood-injection.

1. Introduction

Deoxyribonuclease I (DNase I) is a specific endonuclease facilitating cleavage of single- and double-stranded DNA during apoptosis. DNA cleavage preferentially occurs at phosphodiester bonds adjacent to pyrimidine nucleotides [1,2]. Recombinant human DNase is an FDA-approved drug, used to improve lung function in cystic fibrosis patients through cleavage of DNA in sputum to reduce its viscosity. DNA also occurs in the matrix of infectious, bacterial biofilms [3], where it is produced by active secretion [4,5] or controlled lysis [6,7]. DNA in bacterial biofilms (or "eDNA") serves many functions [3], amongst which stimulation of horizontal gene transfer in biofilms [8,9], chelation of cations and restricting diffusion of cationic antimicrobials [10,11], bacterial adhesion to substrata [12,13] and maintenance of the structural integrity of biofilms [14,15] through acid-base interactions [16].

eDNA has been found in many different Gram-positive and Gram-negative bacterial strains and species [3]. The role of eDNA in maintaining the structural integrity of infectious biofilms is crucial for the protection of biofilm bacterial inhabitants against antimicrobials and the host immune system. Moreover, this important role of eDNA suggests the use of DNase as a biofilm dispersant either for bacterial detachment or for assisting antibiotic treatment to make a biofilm more penetrable. Most studies geared towards the development of DNase as a biofilm dispersant however, are *in vitro* studies [17–20]. Very few studies have been done that demonstrate *in vivo* benefits of the use of DNase to eradicate or prevent the formation of infectious biofilms. An *in vivo* study into the efficacy of DNase for preventing vaginal colonization in mice yielded only 10-fold lower colonization by *Gardnerella vaginalis* upon colonization in presence of DNase as compared with colonization in absence of DNase [21], which is a far smaller effect than observed in

* Corresponding authors.
E-mail addresses: h.c.van.der.mei@umcg.nl (H.C. van der Mei), h.j.busscher@umcg.nl (H.J. Busscher), shilinqi@nankai.edu.cn (L. Shi).

https://doi.org/10.1016/j.cej.2022.139619
Received 25 May 2022; Received in revised form 2 September 2022; Accepted 3 October 2022
Available online 7 October 2022

most *in vitro* studies [18,22].

In vivo administration of DNase in the blood circulation is hampered by its hydrophobicity [23]. Moreover, despite its high stability allowing storage for at least three years at −20 °C and short-term exposure to high temperatures up to 60 °C [24,25], the terminal half-life time of DNase in blood is extremely short due to inactivation by blood-borne enzymes [26,27]. The terminal half-life time of DNase following intravenous injection in mice, has been found to amount only 4.5 min [28], which is about five- to six-times shorter than the time it takes for self-targeting, pH-responsive PEG/PAE micelles [29] or DCPA-H_2O liposomes [30] to reach an abdominal infection site after tail-vein injection in mice.

Ideally, DNase as a dispersant should be co-administered with antibiotics in the blood-circulation to find its own way and self-target to an infectious biofilm [31,32], while at the same time being protected against inactivation by blood-borne enzymes.

In this paper, we describe the synthesis of a poly(amino ester)-DNase conjugate inside the shell of a micellar nanocarrier composed of poly (ethylene glycol)-*block*-poly(ε-caprolactone) (PEG-*b*-PCL) and poly (ε-caprolactone)-*block*-poly(amino ester) (PCL-*b*-PAE) (Fig. 1). The enzymatic activity of DNase conjugated with PAE in PEG/PAE micelles will be compared with the enzymatic activity and stability in blood of DNase free in solution. In addition, the ability of PEG/PAE-DNase micelles, with ciprofloxacin internally core-loaded, to self-target to infectious staphylococcal biofilms, as well as their ability to disperse biofilms and kill its inhabiting bacteria will be studied *in vitro* and *in vivo*. In view of the approved use of DNase for improving lung function in cystic fibrosis patients, a murine pneumonia was used for *in vivo* studies. Accordingly, the study was carried out using *S. aureus* strains, as one of the most common human pathogens and causative amongst others to nosocomial pneumonia [33].

2. Materials and method

2.1. Materials

Monomethoxy PEG (CH_3O-PEG-OH; M_w = 2000) was purchased from Fluka (Shanghai, China) and dried under vacuum before use. ε-Caprolactone (ε-CL; 99 % purity), purchased from Alfa Aesar (Shanghai, China), was dried with calcium hydride and distilled under vacuum conditions. Stannous octoate ($Sn(Oct)_2$; 95 % purity) was purchased from J&K (Beijing, China) and used as received. DNase I from bovine pancreas (≥2,000 units/mg protein) was purchased from Aladdin (Shanghai, China). Proteinase K (40 units/mg protein) was purchased from Meryer (Shanghai, China). All other materials and solvents were used as received without further purification from commercial suppliers, except for chloroform ($CHCl_3$), which was dried over calcium hydride and distilled before use. All aqueous solutions were prepared with ultrapure water (resistance, >18 MΩ/cm) from a Milli-Q system.

2.2. Synthesis of block copolymers

PEG-*b*-PCL was synthesized as previously reported [29]. PCL-*b*-PAE was synthesized by a Michael-type addition polymerization of PCL

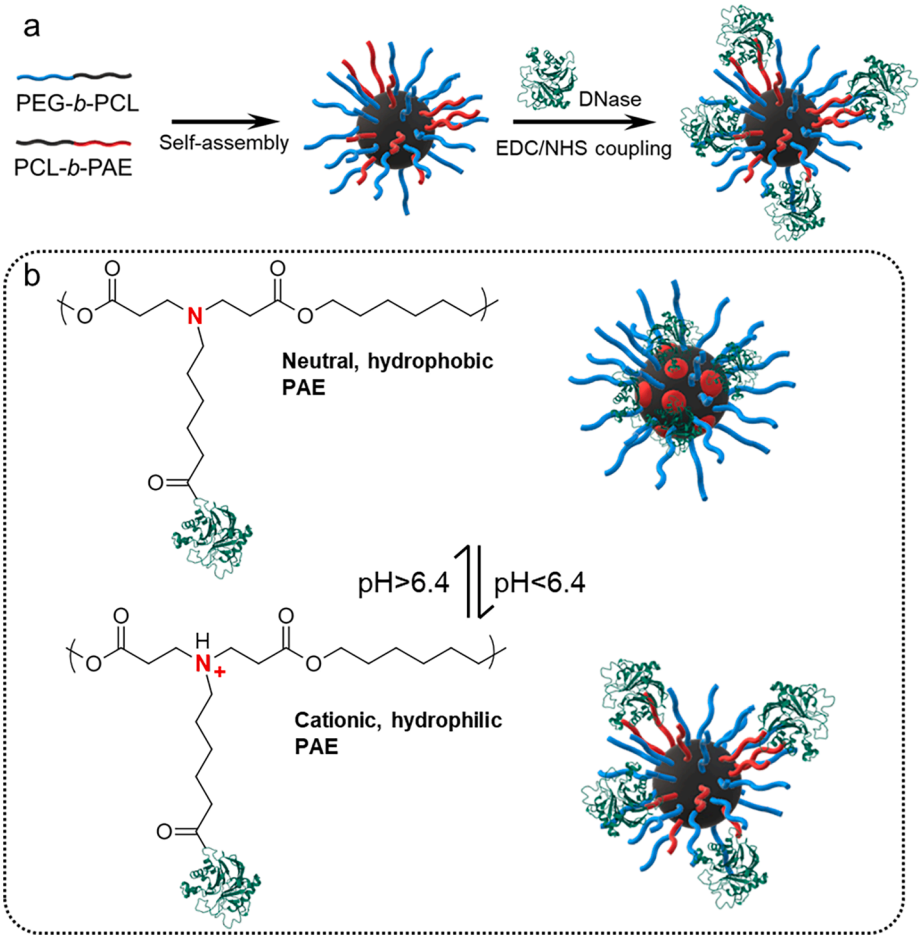

Fig. 1. Synthesis of PEG/PAE-DNase micelles and their pH-responsiveness. (a) PEG-*b*-PCL and PCL-*b*-PAE self-assemble to form PEG-PAE micelles after which DNase is conjugated to amino groups of PAE through 1-ethyl-3-(3-dimethylaminopropyl)carbodiimide/*N*-hydroxysuccinimide (EDC/NHS) coupling at acidic pH. (b) At physiological pH (pH 7.4), DNase is protected in the micellar shell, while at pH < 6.4, PAE becomes positively-charged and stretches to expose the DNase.

monoacrylate, hexane-1,6-dioldiacrylate (HDD), and aminocaproic acid (Fig. S1a). PCL monoacrylate (2.5 g, 0.5 mmol), HDD (2.602 g, 11.5 mmol), and aminocaproic acid (1.574 g, 12 mmol) were weighed and dissolved into 15 mL of anhydrous $CHCl_3$ and methanol mixed solvents in a round-bottom flask. Polymerization was performed at 55 °C under a dry argon atmosphere for 72 h. ^{1}H NMR identified the polymer prepared as PEG_{45}-*b*-PCL_{42} (Fig. S1b) PCL_{44}-*b*-PAE_{18} (Fig. S1c).

2.3. Micelle preparation and characterization

PEG/PAE micelles were prepared through nanoprecipitation as described before [34]. PEG-*b*-PCL and PCL-*b*-PAE were dissolved in dimethyl sulfoxide as stock polymer solutions with a concentration of 5 mg/mL. For the preparation of PEG/PAE micelles, 1 mL of PEG-*b*-PCL stock solution was mixed with 1 mL of PCL-*b*-PAE stock solution, with an equal weight ratio of PEG-*b*-PCL and PCL-*b*-PAE (1:1). The resulting solution was added dropwise to 6 mL of potassium phosphate buffer (pH around 5.5, 10 mM) at 30 s intervals under stirring with a magnetic bar. After stirring for 2 h, the solution was transferred to a dialysis bag (molecular weight cutoff, 3500 Da) and dialyzed against phosphate buffered saline (PBS, 5 mM K_2HPO_4, 5 mM KH_2PO_4, 150 mM NaCl) at pH 7.4 for 2 days.

For the preparation of PEG/PAE-DNase micelles, the above procedure was followed with minor modification. After PEG/PAE micelles had been formed, 1-(3-dimethylaminopropyl)-3ethylcarbodiimide hydrochloride (EDC, 0.96 mg) and *N*-hydroxysuccinimide (NHS, 0.86 mg) were dissolved in PBS (pH 5.0) and added into a PEG/PAE micelles suspension and stirred for 30 min. Then, 0.5 mL of DNase solutions in different concentrations (0.5, 1, 2 and 4 mg/mL) was added, corresponding with feed ratios of DNase to polymer of 1:20, 1:10, 1:5 and 1:2.5. The mixture was allowed to react for 12 h after which PEG/PAE-DNase micelles were harvested as described above. The concentration of DNase conjugated to PAE in the micelles formed was determined using a bicinchoninic acid protein assay kit (Solarbio, Beijing, China) and DNase conjugation content and efficiency were calculated as:

$$\text{DNase conjugation content(wt\%)} = \frac{W_{conjugated\ DNase}}{W_{conjugated\ DNase\ and\ polymer}} \times 100\% \quad (1)$$

$$\text{DNase conjugation efficiency(wt\%)} = \frac{W_{conjugated\ DNase}}{W_{DNase\ in\ feed}} \times 100\% \quad (2)$$

in which $W_{conjugated\ DNase}$ is the weight of DNase conjugated to PAE, $W_{conjugated\ DNase\ and\ polymer}$ is the total weight of DNase conjugated to PAE and polymers and $W_{DNase\ in\ feed}$ is the weight of DNase added to the reaction. Based on optimizing DNase conjugation content and efficiency, a suitable feed ratio of DNase to polymer was determined.

For ciprofloxacin-loading of micelles, micelles were synthesized as described above while adding ciprofloxacin hydrochloride in DMSO (0.5 mL) at different concentrations (0.5, 0.67, 1, 1.25, 2 and 2.5 mg/mL) during micelle formation. These concentration ratios corresponded with feed ratios of ciprofloxacin to polymer of 1:20, 1:15, 1:10, 1:8, 1:5 and 1:4, respectively. Drug loading content of ciprofloxacin were calculated as:

$$\text{DLC(wt\%)} = \frac{W_{loaded\ Cip}}{W_{loaded\ Cip\ and\ polymer}} \times 100\% \quad (3)$$

in which $W_{loaded\ Cip}$ is the weight of ciprofloxacin loaded in micelles and $W_{loaded\ Cip\ and\ polymer}$ is the total weight of ciprofloxacin loaded in micelles and polymers. In order to determine the release of ciprofloxacin from micelles, 2 mL of freshly prepared ciprofloxacin loaded micelles was transferred into a dialysis bag (molecular weight cutoff, 8000 Da), and immersed into 20 mL of PBS (pH 5.0 or pH 7.4) at 37℃. At different time points up to 24 h, 1 mL of the dialysis solution was taken out and the absorbance of the solution at 277 nm was measured by a UV–vis spectrophotometer (UV-1800, Shimadzu, Japan). Based on optimizing the drug loading content and release, a suitable feed ratio of ciprofloxacin to polymer was determined.

Micelles were further characterized by Dynamic Light Scattering (DLS) to determine their diameters. DLS was done at a 90°scattering angle at 37 °C with a 636 nm laser light scattering spectrometer (BI-200SM), equipped with a digital correlator (BI-10000AT). Zeta potentials of micelles were measured in PBS as a function of pH (5.0 to 7.4) using a Brookhaven ZetaPALS (Brookhaven Instrument, USA). The instrument uses phase analysis scattered light at 37 °C to provide an average zeta potential over multiple particles. Micelles were visualized using Transmission Electron Microscopy (TEM; Talos F200C, FEI, USA) at an acceleration voltage of 200 kV. Samples were prepared for TEM by dropping a micelle suspension onto a carbon-coated copper grid and slow drying *in vacuo* at room temperature.

To investigate the pK_a of PAE, titration and turbidity experiments were performed according to a previous report [35]. Briefly, 2 mg of PCL-*b*-PAE solved in 1 mL of DMSO dropwise to 6 mL in HNO_3 solution (pH ~ 3.0). Then, the pH value of the solutions was adjusted to 3. Subsequently, pH value and turbidity were recorded upon addition of NaOH solution (0.1 M).

2.4. Enzymatic activity of DNase

Enzymatic activity of PEG/PAE-DNase micelles was evaluated by monitoring the changes of absorbance at 260 nm at 37℃. To this end, calf thymus DNA (Sigma, Shanghai, China) was dissolved in Tris-HCl buffer (10 mM, pH 7.4). Next, 400 μL DNase or PEG/PAE-DNase micelles were mixed with 40 μL DNA (250 μg/mL) at equal DNase equivalent concentrations (40 μg/mL), supplemented with $MgCl_2$ (25 mM) and $CaCl_2$ (5 mM). Absorbances (260 nm) were monitored with a UV–vis spectrophotometer.

2.5. Stability of DNase in vitro and in vivo

To study the stability of DNase in PEG/PAE-DNase micelles under different conditions, the enzymatic activity of DNase and PEG/PAE-DNase were evaluated and compared as described above. *In vitro* stability of DNase or PEG/PAE-DNase at an equal DNase equivalent concentration (40 μg/mL) was studied (1) after 1 h exposure 65 °C, (2) after incubation for 8 h with proteinase K at 37 °C and (3) after storage for seven days at 4 °C in PBS.

For evaluating the stability of DNase in PEG/PAE-DNase micelles *in vivo*, four- to five-week-old healthy female BALB/c nude mice were purchased from HFK Bioscience Co., ltd. (Beijing, China) and subjected to experiments in accordance with the Guidelines for Care and Use of Laboratory Animals of Nankai University. Experiments were approved by the Animal Ethics Committee of Nankai University (Tianjin, China). Mice were randomly divided into two groups (n = 3) and tail-vein injected with RhB-labeled DNase or RhB-labeled PEG/PAE-DNase micelles in PBS at DNase equivalent concentrations 40 μg/mL. Blood samples were collected at different time points after injection and centrifuged at 4000 rpm for 10 min at 4℃ to remove the blood cells. Plasma fractions were collected and their fluorescence measured at 575 nm upon excitation at 543 nm and DNase presence calculated as a percentage fluorescence with respect to the fluorescence of the injected dose.

2.6. Bacteria culturing and harvesting

Green fluorescent protein (GFP) expressing *S. aureus* ATCC12600^{GFP} [36] and bioluminescent *S. aureus* Xen36 were employed in this study, cultured and harvested as described before [34]. *S. aureus* ATCC12600 is isolated from human pleural fluid [37], while *S. aureus* Xen36 was derived from the parental strain *S. aureus* ATCC49525 (Wright), a clinical isolate from a bacteremia patient [38]. The strains were cultured from a frozen stock onto tryptone soy agar plates supplemented with tetracycline (10 μg/mL) for *S. aureus* ATCC12600^{GFP} and kanamycin

(200 μg/mL) for *S. aureus* Xen36 at 37 °C in ambient air. For experiments, one colony was transferred to inoculate 10 mL of tryptone soya broth (TSB, Oxoid, Basingstoke, UK), additional supplemented with tetracycline (10 μg/mL) for *S. aureus* ATCC12600^{GFP}, at 37 °C for 24 h in ambient air. This preculture was diluted 1:20 in 100 mL of TSB and grown statically for 16 h at 37 °C. Cultures were harvested by centrifugation for 5 min at 5000g at 10 °C, washed twice in PBS, and lastly suspended in 10 mL of PBS to a concentration of 3×10^8 bacteria per mL, as determined in a Bürker-Türk counting chamber.

2.7. Biofilm formation

For biofilm formation, 500 μL of a staphylococcal suspension (3×10^8 bacteria per mL) was added in 48-well microplates or 20 mm glass bottom confocal dishes for 1.5 h at 37 °C under static condition. Then, PBS was removed and the wells were gently washed three times with PBS to remove planktonic bacteria. TSB medium was added into the plates and incubated at 37 °C under static condition for 48 h, refreshing the medium after 24 h. Biofilms of *S. aureus* ATCC12600^{GFP} and *S. aureus* Xen36 were grown for 48 h before further experiments.

2.8. Penetration and accumulation of micelles in biofilms

To study the penetration and accumulation of micelles in biofilms, Rhodamine B fluorescence (RhB) labeled DNase (DNase-RhB) was used. 0.25 mg of Rhodamine B isothiocyanate was reacted with 5 mg of DNase in 100 mM $NaHCO_3$ buffer (pH 9.5) under stirring at 4 °C for 12 h in the dark. Excess RhB was removed by dialysis against PBS at 4 °C. For the fluorescent labeling of PEG/PAE-DNase micelles, PEG/PAE-DNase micelles were prepared as described above using RhB-labeled DNase was used. *S. aureus* ATCC12600^{GFP} biofilms were grown in sterile 20 mm glass bottom confocal dishes as described above and exposed to RhB-labeled DNase or PEG/PAE-DNase micelles in PBS at pH 5.0. After 30 min, exposed biofilms were rinsed gently with buffer and observed using confocal laser scanning microscopy (CLSM, Nikon, A1+, Japan). Images were quantitatively analyzed using ImageJ software. In order to compare penetration and accumulation of PEG/PAE-DNase micelles with PEG/PAE micelles, PEG/PAE micelles were loaded with red-fluorescent Nile red. The further experimental procedure was identical as for RhB-labeled DNase or PEG/PAE-DNase micelles. All experiments were carried out in triplicate with separate grown biofilms.

2.9. Degradation of eDNA in staphylococcal biofilm

The amount of eDNA in *S. aureus* Xen36 biofilms was quantified by PicoGreen dsDNA assay kit (Yeasen, Shanghai, China), as previously described [39]. Biofilms grown in 48 well plates as described above, were exposed for 4 h to DNase in solution, PEG/PAE or PEG/PAE-DNase micelles (500 μL, at a DNase equivalent concentration of 40 μg/mL). Then, biofilms were gently rinsed three times with PBS and resuspended with Tris-EDTA buffer (10 mM Tris, 1 mM EDTA, pH 7.5). Next the amount of eDNA in a biofilm was measured according to manufacturer's instructions, using calibration curves generated by serial dilution of λDNA solution provided in the kit. All measurements were carried out in triplicate with separately grown biofilms.

2.10. Dispersal of staphylococcal biofilms

Biofilm mass was determined using a crystal violet (CV) assay. *S. aureus* ATCC12600^{GFP} biofilms grown in 48-well microplates as described above, were exposed for 4 h to DNase, PEG/PAE or PEG/PAE-DNase micelles (500 μL, at a DNase equivalent concentration of 40 μg/mL). Subsequently, 500 μL of a CV solution (1 %, w/v) was added to each well to stain the biofilms for 20 min. Next, CV solution was removed and wells were gently rinsed three times with PBS. After rinsing, 500 μL of 33 % acetic acid was added for 15 min to dissolve the stained biofilm and absorbance in each well was read on a microplate reader (Spark, Tecan, Switzerland) at 595 nm. Each assay was carried out in triplicate with separately grown biofilms.

Biofilms grown on glass sides in 48-well plates as described above, were also examined after exposure using Scanning Electron Microscopy (SEM). After exposure and washing, biofilms were fixed with 2.5 % glutaraldehyde for 2 h at 4 °C, dehydrated with a series of ethanol solutions and gold sprayed for SEM (Quanta 200, FEI, Hillsboro, USA) at an acceleration voltage of 15 kV and a magnification of 10000×.

2.11. Killing of staphylococci in their biofilm mode of growth

S. aureus ATCC12600^{GFP} biofilms grown for 48 h in 48-well microplates as described above, were exposed to ciprofloxacin hydrochloride in solution, a mixture of DNase and ciprofloxacin, ciprofloxacin loaded PEG/PAE or PEG/PAE-DNase micelles at equivalent ciprofloxacin concentrations of 0, 10, 20, 40 and 80 μg/mL for 4 h. Biofilms viability was assessed from the green-fluorescence of biofilms as measured with the microplate reader. In addition, the number of colony forming units (CFU) in the biofilms was enumerated after exposure. To this end, biofilms were scraped off the well surface and bacteria were suspended in PBS. The suspensions were sonicated and subsequently serially diluted in PBS. 50 μL of each dilution was plated on TSB agar plates and incubated for 24 h at 37 °C and the numbers of CFUs were counted. The experiments were carried out in triplicate with separately grown biofilms.

2.12. Self-targeting of PEG/PAE-DNase micelles and eradication of staphylococcal pneumonia in mice

First, a staphylococcal pneumonia model was set up in mice. Staphylococci were chosen for infection, as staphylococci represent the number one causative strain for nosocomial pneumonia [40]. To this end, female BALB/c nude mice were anesthetized with isoflurane and intranasally infected with *S. aureus* ATCC12600^{GFP} suspension (10^9 bacterial per mL, 50 μL) [41,42]. Establishment of infection was verified using a bio-optical imaging system (IVIS Lumina II, Imaging System, PerkinElmer) on excised lungs (Fig. S7). Body weight and survival were measured daily.

For studying self-targeting, staphylococcal pneumonia infected mice were tail-vein injected with DNase-RhB and PEG/PAE-DNase-RhB micelles (200 μL at a DNase equivalent concentration of 40 μg/mL). At 4 h post-injection, mice were sacrificed, and major organs were harvested. *Ex vivo* imaging was conducted by a bio-optical imaging system.

For studying eradication of pneumonia, staphylococcal pneumonia infected mice were randomly divided into five groups (n = 6). Mice were injected intravenously with PBS, ciprofloxacin in PBS (10 mg/kg), a mixture of DNase (0.1 mg/kg) and ciprofloxacin (10 mg/kg), ciprofloxacin loaded PEG/PAE (25 mg/kg) or PEG/PAE-DNase micelles (25 mg/kg). The body weight of each mouse and the number of surviving mice were recorded daily. At the end of treatments, mice were sacrificed. Lungs were collected, homogenized, serially diluted, plated on TSB agar plates, and after 18 h of incubation at 37 ℃, the CFUs were counted. The levels of TNF-α and IL-6 within the lungs were assessed by a mouse TNF-α and IL-6 ELISA kits (BD Biosciences, America) according to the manufacturer's protocols, respectively.

2.13. Tissue and blood compatibility of ciprofloxacin-loaded PEG/PAE-DNase micelles in vivo

Histological evaluation and blood analyses were performed to evaluate biocompatibility of ciprofloxacin loaded PEG/PAE-DNase micelles *in vivo*. Major organs (hearts, lung, liver, spleen, and kidney) were collected at the end of treatment, followed by hematoxylin and eosin staining and microscopic examination.

At day 4 and day 9, blood samples were collected from eyes of mice

intravenously injected with ciprofloxacin loaded PEG/PAE-DNase micelles for hematological analysis.

2.14. Statistical analysis

All data are expressed as means ± SD (Standard Deviation). Statistical significances between two groups were examined using a Student's *t* test. Multivariate parametric data were analyzed using analysis of variance (ANOVA) using a Tukey's post hoc test.

3. Results

3.1. Preparation and characterization of micelles

First, PEG/PAE micelles were fabricated by self-assembly of block copolymers of PEG-*b*-PCL and PCL-*b*-PAE (see Fig. S1 for synthesis of block copolymers). The critical micelle concentration (CMC, total polymer concentration) of a solution with equal concentrations of both block polymers amounted 6.1 μg/mL (Fig. S2). Accordingly, PEG/PAE micelles were prepared by self-assembly of a solution with a total polymer concentration of 500 μg/mL, i.e. well above CMC.

Bovine pancreatic DNase was used for conjugation, possessing 10 residual amino groups (Fig. S3) for conjugation to PAE through EDC/NHS chemistry. Conjugation of DNase was verified using fluorescence spectroscopy. DNase showed a major fluorescence emission at 333 nm due to residual tyrosine [43], that is fully absent in PEG/PAE micelles but clearly observable in PEG/PAE-DNase micelles (Fig. 2a). This confirms successful conjugation of DNase to PEG/PAE micelles. DNase conjugation content and efficiency were assessed using a bicinchoninic acid assay and both depended on the micelle to DNase feed ratio during conjugation (Fig. 2b). Conjugation efficiency decreased with increasing feed ratio, while conjugation content increased. Since efficiency continued to decrease above a feed ratio of 1:10, to fully utilize DNase, a DNase to a micelle feed ratio of 1:10 was employed for further experiments. Far-UV circular dichroism spectra were similar for DNase and PEG/PAE-DNase micelles, implying that the DNase structure was not influenced by PAE-conjugation (Fig. S4). Both PEG/PAE and PEG/PAE-DNase micelles had a spherical morphology (Fig. 2c) with small polydispersity indices. The hydrodynamic diameters of PEG/PAE (Fig. 2d) as well as of PEG/PAE-DNase (Fig. 2e) micelles were <90 nm and distributed within a narrow range, regardless of pH and DNase loading. PEG/PAE and PEG/PAE-DNase micelles had negative zeta potentials around −5 mV at pH 7.4, while becoming positive at pH 5.0 (around + 9 mV) (Fig. 2f). Titration experiments confirmed that PCL-*b*-PAE (Fig. 3a) and PCL-*b*-PAE-DNase (Fig. 3b) became protonated below pH 6.4. Charge reversal due to protonation at pH 6.4, was accompanied by an increase in UV-transmittance of PCL-*b*-PAE (Fig. 3c) and PCL-*b*-PAE-DNase (Fig. 3d) solutions. The increase in transmittance at acidic pH indicate increased hydrophilicity of PAE, allowing its stretching and yielding a higher water content of the micelles and accordingly a clearer solution resulted than at pH 7.4. In line, micellar diameters slightly increased in an acidic environment as compared with pH 7.4 (compare Fig. 2d, e) due to stretching of PAE.

3.2. Enzymatic activity of PAE-conjugated DNase

Enzymatic degradation of DNA was monitored using UV–vis spectroscopy. Intact DNA demonstrated an absorption band at 260 nm that

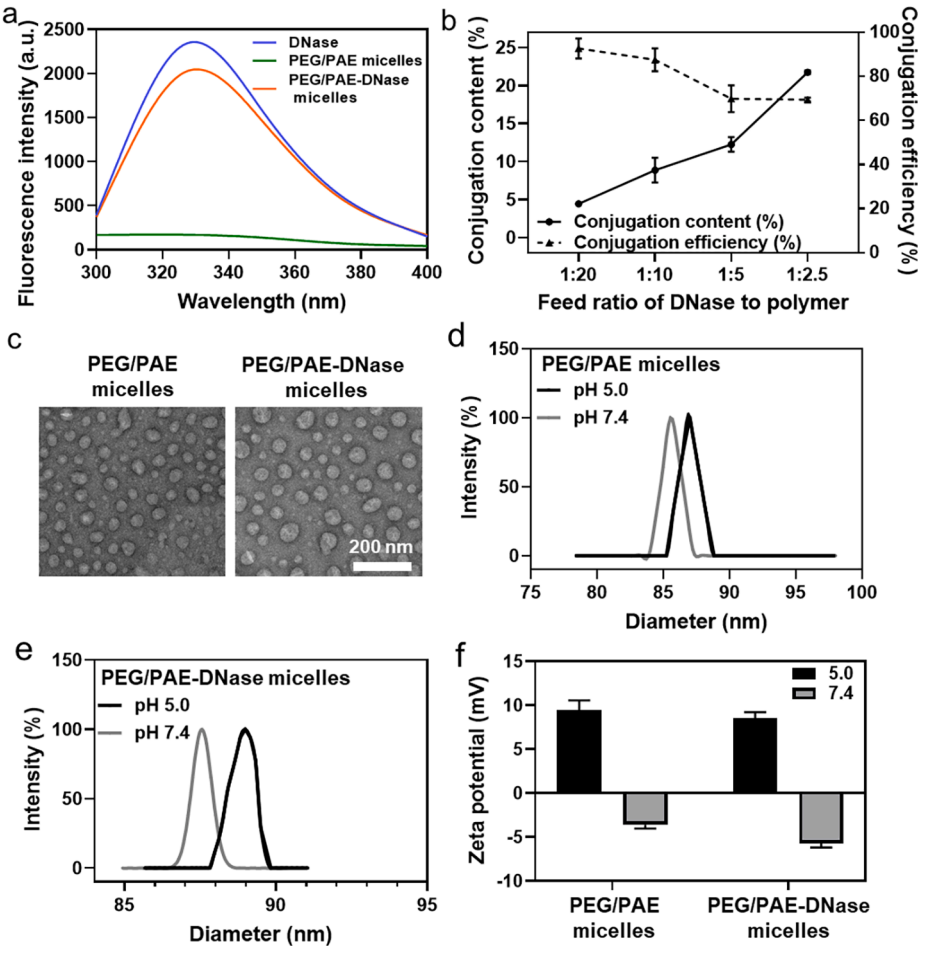

Fig. 2. Characterization of PEG/PAE micelles with and without PAE-conjugated DNase. (a) Fluorescence spectra of DNase and micelles. The excitation wavelength was at 276 nm. (b) The conjugation content and efficiency of DNase to micelles as a function of the feed ratio of micelles to DNase (by weight). (c) TEM micrographs of micelles. (d) Hydrodynamic diameter distribution of PEG/PAE micelles at pH 5.0 (mean 88 nm, polydispersity index 0.22) and 7.4 (mean 85 nm, polydispersity index 0.21). (e) Same as panel (d), now for and PEG/PAE-DNase micelles at pH 5.0 (mean 89 nm, polydispersity index 0.27) and 7.4 (mean 88 nm, polydispersity index 0.25). (f) Zeta potentials of micelles measured in PBS (37 °C) at pH 5.0 and 7.4. All error bars denote standard deviations over three separately prepared batches of micelles.

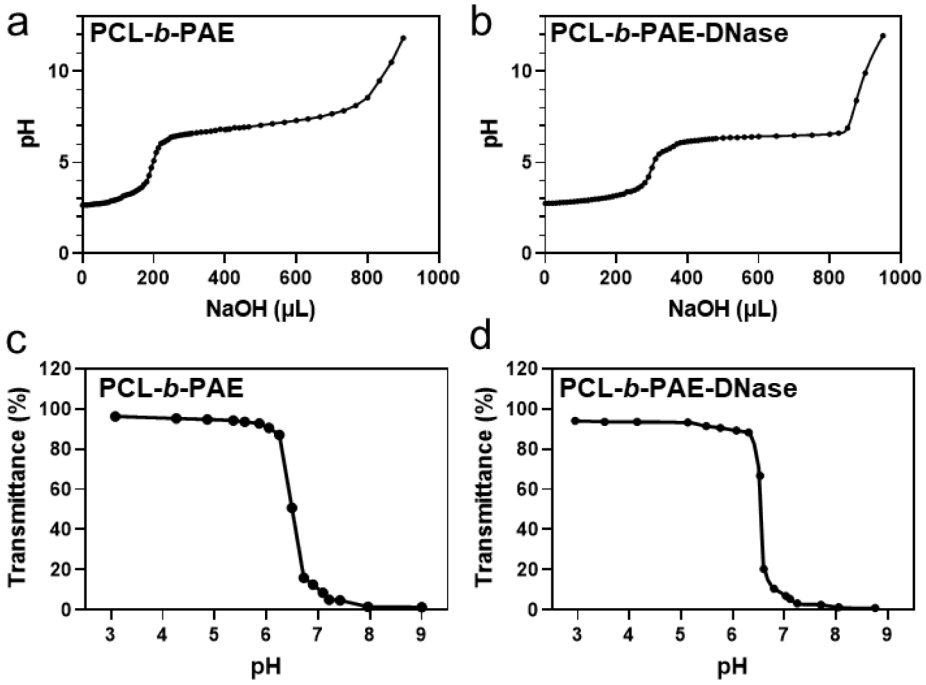

Fig. 3. Protonation and hydrophilization in PCL-*b*-PAE and PCL-*b*-PAE-DNase in relation with pH changes. (a) pH of a PCL-*b*-PAE solution (250 μg/mL) in HNO_3 (pH 3) as a function of the amount of NaOH added (0.1 M). (b) Same as panel (a), now for a PCL-*b*-PAE-DNase solution. (c) UV-transmittance at 550 nm of PCL-*b*-PAE solution (250 μg/mL) in HNO_3 (pH 3) as a function of pH. (d) Same as panel (c), now for a PCL-*b*-PAE-DNase solution.

increased upon enzymatic degradation in presence of DNase due to deoxyribonucleoside monophosphates (Fig. 4a). Accordingly, increases in absorbance at 260 nm were taken indicative of DNA degradation. Exposure of a DNA solution to PEG/PAE micelles during 1 h yielded no degradation of DNA, while 1 h exposure to DNase caused 96 % degradation (Fig. 4b), both regardless of pH. Degradation caused by exposure to PEG/PAE-DNase micelles yielded less degradation than a DNase solution and was pH-dependent. Degradation by PEG/PAE-DNase micelles was higher at pH 5.0 than at pH 7.4, likely due to the stretching of PAE at low pH bringing PAE-conjugated DNase molecules that are, at pH 7.4, contained in the micellar shell further outwards.

3.3. *Protective conjugation of DNase to PAE in vitro and in vivo*

In-shell protection of DNase through conjugation with PAE in PEG/PAE-DNase micelles yielded significant protection against heating (Fig. 5a) and exposure to proteinase K (Fig. 5b) *in vitro*. In order to evaluate in-shell protection of DNase *in vivo*, Rhodamine B isothiocyanate (RhB) was used to label DNase. Fluorescent DNase or PEG/PAE-DNase micelles were tail-vein injected in healthy mice (Fig. 5c). DNase protected in the shell of PEG/PAE-DNase micelles maintained a significantly higher concentration during circulation in blood than when dissolved unprotected in blood (Fig. 5d). Assuming an exponential decrease to zero, terminal half-life times of 2.5 ± 0.2 h and 9.7 ± 0.5 h were calculated for DNase and PEG/PAE-DNase micelles, respectively. Taking the area under the blood concentration–time curve as a measure of bioavailability while assuming an exponential decrease to zero, PEG/PAE-DNase micelles were found to have a bioavailability of 274 ± 5 μg h/mL, which is significantly higher than of DNase (72 ± 4 μg h/mL). The prolonged activity of DNase in PEG/PAE-DNase micelles as compared with DNase free in solution during blood circulation *in vivo* is attributed to the combination of in-shell hiding of DNase and PEG preventing non-specific adsorption of blood-borne proteins during blood circulation at physiological pH [44]. Note that also the shelf-life of DNase during storage in PBS under ambient conditions increased when contained in-shell (Fig. S5).

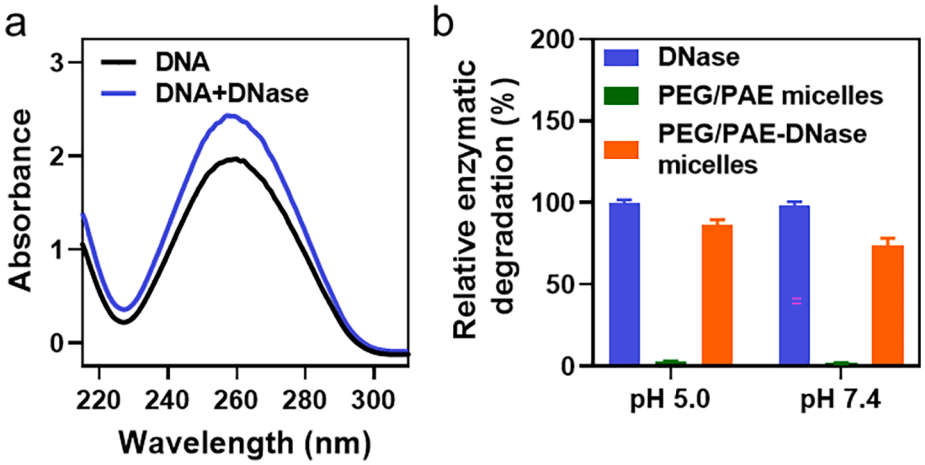

Fig. 4. Enzymatic activity of PEG/PAE micelles with and without PAE-conjugated DNase. (a) UV–vis absorption spectrum of DNA solution in PBS (pH 7.4) with and without exposure to DNase (40 μg/mL). Spectrum taken after 60 min exposure to DNase. (b) Enzymatic degradation of DNA (250 μg/mL) upon 1 h exposure to DNase, PEG/PAE or PEG/PAE-DNase micelles (equivalent DNase concentration: 40 μg/mL in PBS) at pH 5.0 or 7.4. Enzymatic degradation was expressed relative to the absorbance change at 260 nm of a DNA solution exposed to DNase (pH 7.4). All error bars denote standard deviations over three separately prepared batches of micelles.

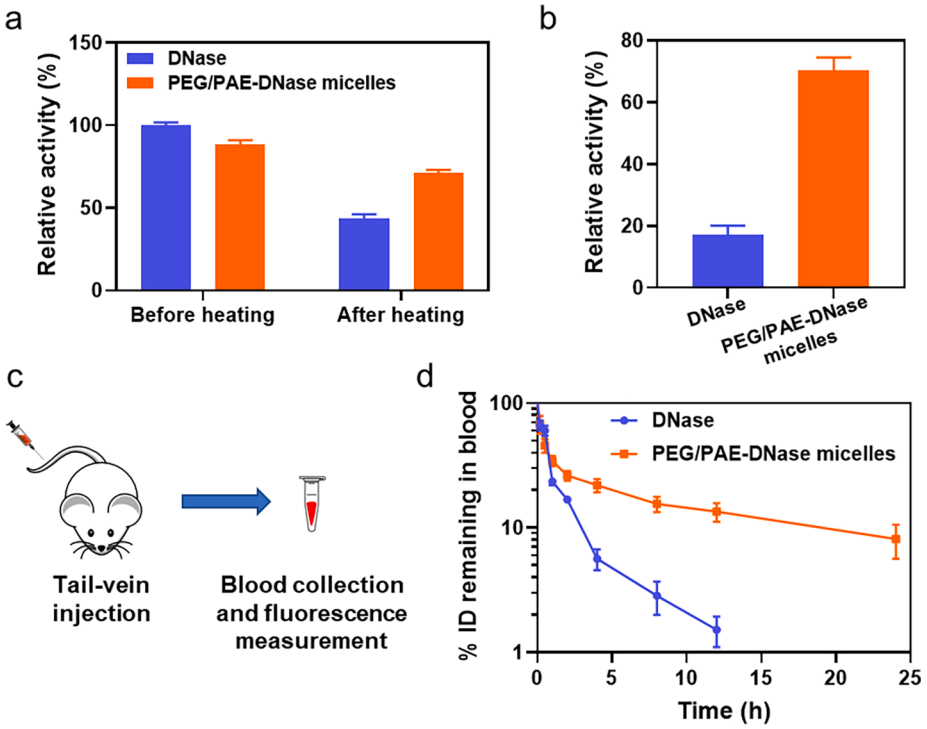

Fig. 5. In-shell protection of DNase in PEG/PAE-DNase micelles *in vitro* and *in vivo*. (a) Enzymatic activity of DNase and PEG/PAE-DNase micelles in PBS (pH 7.4) after heating at 65°C for 1 h, expressed relative to the enzymatic activity of a freshly prepared DNase solution (DNase or DNase-equivalent concentrations 40 μg/mL). All error bars denote standard deviations over three separately prepared batches of micelles. (b) Same as panel a, now measuring relative activity after 8 h exposure to Protease K. (c) Workflow for RhB-labeled DNase or micelles injection in the tail-vein of mice, followed by blood sample collection and fluorescence measurement. (d) Percentage concentration of DNase *in vivo* as a function of time after tail-vein injection in mice for RhB-labeled DNase dissolved in blood or protected in the shell of PEG/PAE-DNase micelles suspended in blood (DNase or DNase equivalent concentrations 40 μg/mL). Percentage concentration of DNase in blood was expressed as a percentage with respect to the fluorescence of RhB-labeled DNase of the injected dose (% ID). All error bars denote standard deviations over experiments carried out in a group of three mice.

3.4. Penetration and accumulation of micelles in biofilms in vitro and in vivo

Penetration and accumulation into biofilms of green-fluorescent *Staphylococcus aureus* ATCC12600^{GFP} was studied using red-fluorescent RhB-labeled DNase and PEG/PAE-DNase micelles. DNase dissolved in PBS only penetrated the surface region of the staphylococcal biofilms regardless of pH (see Fig. 6a for CLSM images), probably due to slow and minor degradation of eDNA in the biofilm matrix. PEG/PAE-DNase micelles were also unable to penetrate staphylococcal biofilms at pH 7.4, but at pH 5.0 PEG/PAE-DNase micelles were found accumulated over the depth of a biofilm. Quantitative analysis confirmed accumulation of PEG/PAE-DNase micelles over the depth of a biofilm at pH 5.0 (Fig. 6b) as well as a higher total accumulation (Fig. 6c). Penetration into the staphylococcal biofilm proceeded slightly faster for PEG/PAE-DNase micelles than for PEG/PAE micelles (Fig. S6).

In order to investigate penetration and accumulation of micelles in infected lungs *in vivo*, a staphylococcal-pneumonia murine model was employed. Two days after infection mice, intranasally infected with *S. aureus* ATCC12600^{GFP}, expressed clear green-fluorescence in the lungs that was absent in an uninfected control group (Fig. S7). This confirmed successful formation of a staphylococcal biofilm in the lungs.

Unlike RhB-labelled DNase, tail-vein injected RhB-labeled PEG/PAE-DNase micelles found their way in the blood circulation of mice towards staphylococcal biofilm in murine lungs within 4 h after injection (see Fig. 6d for fluorescence images and Fig. 6e for quantitative analysis).

3.5. eDNA degradation and dispersal of staphylococcal biofilms by PEG/PAE-DNase micelles in vitro

The ability of PEG/PAE-DNase micelles to degrade eDNA in staphylococcal biofilms and biofilm dispersal was evaluated *in vitro*. eDNA degradation in *S. aureus* Xen36 biofilms was measured using a PicoGreen assay after preparation of a calibration curve (Fig. S8). The amount of eDNA in the matrix of staphylococcal biofilms was reduced threefold and twofold upon exposure to PEG/PAE-DNase micelles and DNase, respectively, compared with exposure to PBS (Fig. 7a). Moreover, PAE-conjugated DNase in micelles reduced the amount of eDNA significantly better than DNase free in solution.

Next, dispersal of biofilms was determined using a crystal violet assay. Upon exposure to PEG/PAE-DNase micelles, total biomass was significantly reduced to 29 %, relative to exposure to PBS. This is twofold better than achieved upon exposure to DNase yielding a reduction of only 57 % (Fig. 7b). Bacterial detachment from biofilms into supernatant due to the degradation of matrix eDNA was significantly higher in supernatants of staphylococcal biofilms exposed to DNase in solution or a suspension of PEG/PAE-DNase micelles than upon exposure to PBS or PEG/PAE micelles without conjugated DNase (Fig. 7c). SEM micrographs confirmed a more open structure and lower density of adhering bacteria in biofilm remaining after exposure to PEG/PAE-DNase micelles compared with exposure to PBS, PEG/PAE micelles or DNase in solution (Fig. 7d).

3.6. Ciprofloxacin loading of PEG/PAE-DNase micelles

Ciprofloxacin-loaded PEG/PAE-DNase micelles were fabricated by self-assembly as described above, but this time in presence of ciprofloxacin. The drug loading content of both PEG/PAE as well as of PEG/PAE-DNase micelles increased with the feed ratio of ciprofloxacin to polymers (Fig. 8a). However, when the feed ratio increased above 1:5, the increase in drug loading content was minor and hence for further studies ciprofloxacin loading of micelles was done at feed ratio of 1:5. The average hydrodynamic diameter of micelles upon ciprofloxacin loading was slightly larger than of unloaded micelles and amounted 96 nm and 90 nm at pH 5.0 and pH 7.4, respectively (Fig. S9a). The pH-response of the zeta potentials of ciprofloxacin-loaded and unloaded micelles was also similar (Fig. S9b). Release of ciprofloxacin was similar from PEG/PAE and PEG/PAE-DNase micelles (Fig. 8b). Cumulative release of ciprofloxacin was higher at pH 5.0 than at pH 7.4, possibly due to enhanced solubility of ciprofloxacin at acidic pH [45] but nevertheless confined to 40 % due to the zwitterionic structure of ciprofloxacin. At pH 7.4, ciprofloxacin is negatively charged and hydrophobic and interacts with the hydrophobic micellar core, while PAE-blocks are collapsed on the micellar core, hindering the release of ciprofloxacin. At

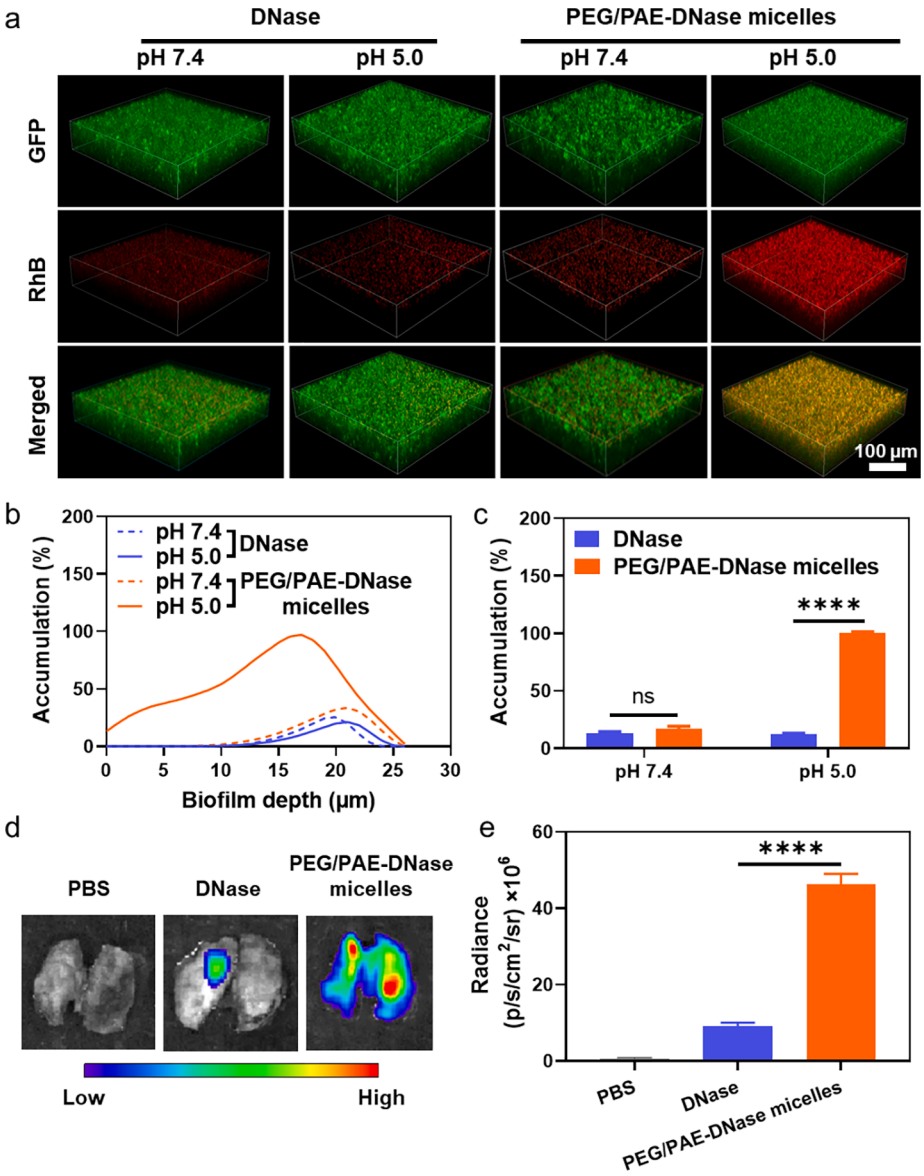

Fig. 6. Penetration and accumulation of PEG/PAE-DNase micelles in *S. aureus* ATCC12600^{GFP} biofilms *in vitro* and *in vivo*. (a) 3D overlayer and a transverse, optical cross-sectional images showing accumulation of RhB-labeled DNase and PEG/PAE-DNase micelles into green-fluorescent, 48 h old biofilms after 1 h exposure at different pH in PBS. (b) Percentage accumulation of DNase and PEG/PAE-DNase micelles as a function of biofilm depth. Percentage accumulation was derived from red-fluorescence, after normalization with respect to the maximum red-fluorescent intensity observed for PEG/PAE-DNase micelles at pH 5.0. (c) Same as panel b, now for the total accumulation of DNase and PEG/PAE-DNase micelles in *S. aureus* biofilms. Error bars denote SDs over three experiments with separately prepared micelle batches and differently grown staphylococcal cultures. (d) *Ex vivo* fluorescence imaging of DNase and PEG/PAE-DNase micelle accumulation after self-targeting in infected lungs, explanted 4 h after tail-vein injection of DNase and PEG/PAE-DNase micelles (dose: 200 μL at a DNase equivalent concentration of 40 μg/mL). Fluorescence intensity is expressed on a pseudo-color scale. (e) Fluorescence radiance from the images presented in panel d. Error bars denote SDs over three mice. **** indicates statistically significant differences at $P < 0.0001$ (Student's *t* test). ns, not significant.

pH 5.0, ciprofloxacin is positively charged and its solubility increased. At the same time, PAE becomes positively charged and electrostatically repels positively charged ciprofloxacin molecules. This mechanism confines the release of the ciprofloxacin.

3.7. Eradication of staphylococcal biofilms by ciprofloxacin-loaded PEG/PAE-DNase micelles in vitro and in vivo

The killing efficacy of *S. aureus* ATCC12600^{GFP} in a biofilm mode of growth increased with increasing ciprofloxacin loading up till 80 μg/mL ciprofloxacin (Fig. 9a), the maximal feed ratio possible for PEG/PAE-DNase micelles (1:5). Killing of staphylococci was evaluated *in vitro* by measuring bacterial fluorescence of biofilms and plate counting. Killing efficacy was dependent on the exposure time (Fig. 9b). In addition to deriving killing efficacies from the green-fluorescence arising from staphylcocci (Fig. 9a, b), also CFU enumeration of staphylococci after ciprofloxacin after various modes of expsoure confirmed that ciprofloxacin loaded PEG/PAE-DNase micelles were superior in killing *S. aureus* in biofilms (Fig. 9c), despite confined ciprofloxacin release (Fig. 8b).

For *in vivo* evaluation, a murine pneumonia model was used in which mice were treated according to the schedule in Fig. 10a. Staphylococcal pneumonia led to death of all mice within 8 and 12 days when treated with PBS or ciprofloxacin, respectively (Fig. 10b). When treated with ciprofloxacin-loaded PEG/PAE micelles, one mouse died, while survival was maximal for mice treated with ciprofloxacin-loaded PEG/PAE-DNase micelles. However, whereas all mice survived upon treatment with ciprofloxacin-loaded PEG/PAE-DNase micelles, four mice died when treated with ciprofloxacin and DNase in solution. Concurrently, only mice treated with ciprofloxacin-loaded PEG/PAE or PEG/PAE-DNase micelles did not suffer weight loss during the experimental period (Fig. 10c). Inflammation markers, including TNF-α (Fig. 10d) and IL-6 (Fig. 10e) however, were significantly lower in mice treated with ciprofloxacin-loaded PEG/PAE-DNase micelles, as compared with mice treated with ciprofloxacin loaded PEG/PAE micelles or a solution of ciprofloxacin and DNase. The occurrence of these inflammation markers in the different treatment groups, paralleled the number of *S. aureus* CFUs isolated from the lungs of mice in different treatment groups after sacrifice at day 14 (Fig. 10f). Also histopathologic examination of lung tissues revealed markedly reduced infiltrates of inflammatory cells in mice treated with a combination of ciprofloxacin and DNase, most notably when incorporated in PEG/PAE-DNase micelles (Fig. 9g). In

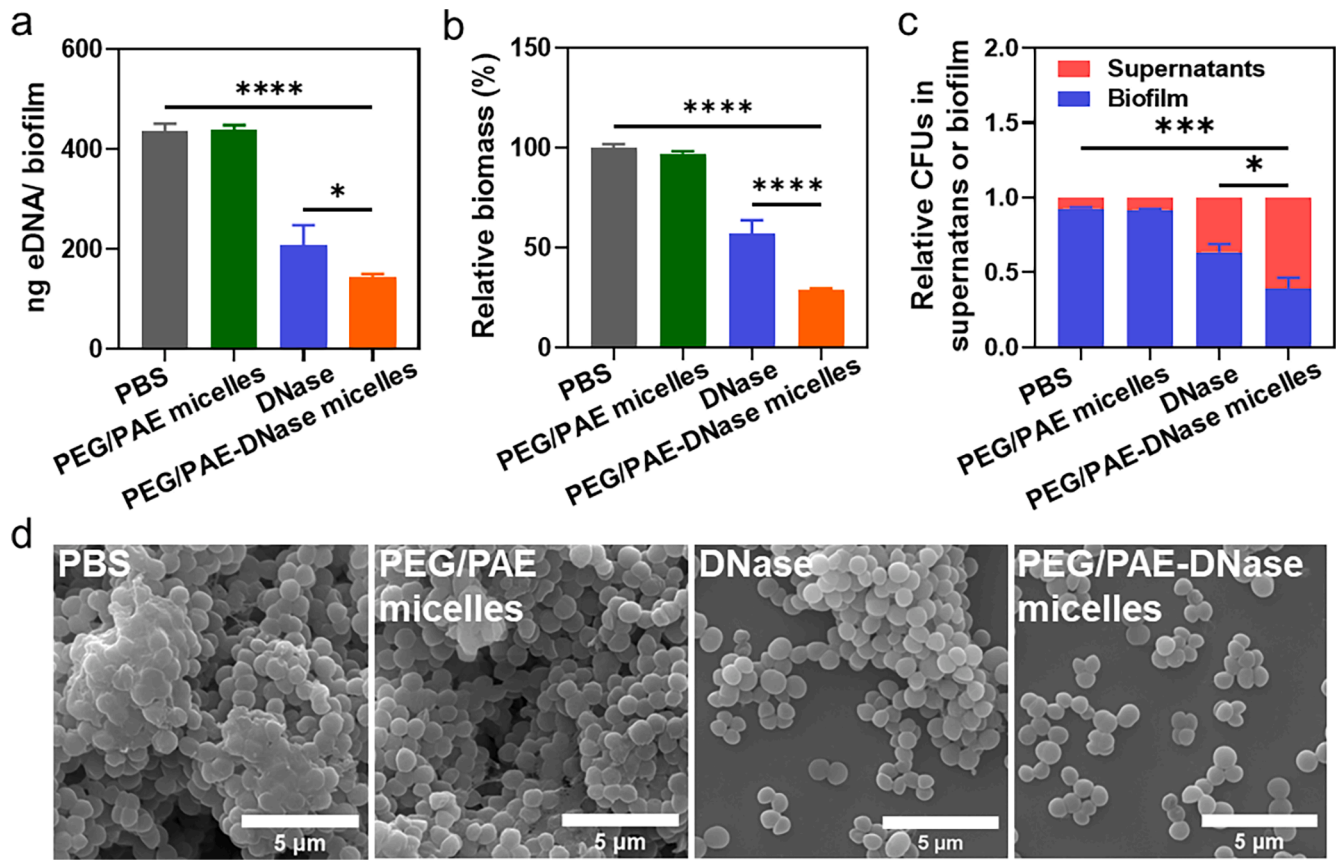

Fig. 7. eDNA degradation and dispersal of *S. aureus* biofilms by PEG/PAE-DNase micelles *in vitro*. (a) eDNA in *S. aureus* Xen36 biofilms after exposure to DNase or micellar suspensions using PicoGreen assay. (b) Biomass of *S. aureus* ATCC12600^{GFP} biofilms determined using crystal violet assay. Bacterial biomass exposed to PBS were set to 100 %. (c) Fraction of CFUs in the supernatants and remaining *S. aureus* ATCC12600^{GFP} biofilms relative to the total number of CFUs retrieved, determined by plate counting. All error bars denote standard deviations over three experiments with separately prepared micelle batches and differently grown staphylococcal cultures. *, *** and **** indicate statistically significant differences at $P < 0.05$, $P < 0.001$ and $P < 0.0001$, respectively (one-way ANOVA or two-way ANOVA). (d) SEM micrographs of 48 h old *S. aureus* ATCC12600^{GFP} biofilms after 4 h of exposure to PBS, DNase, or micellar suspensions of PEG/PAE and PEG/PAE-DNase.

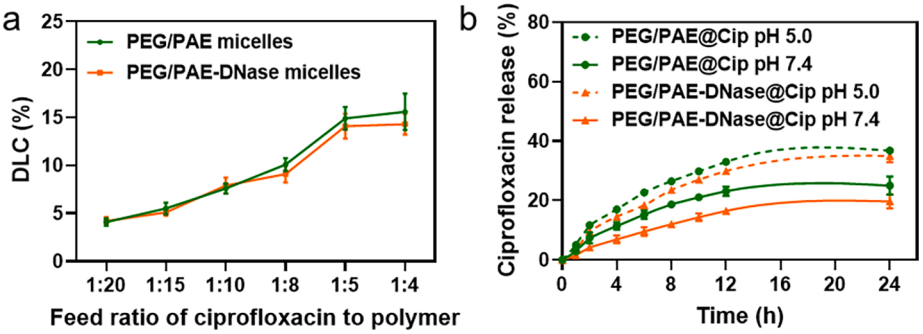

Fig. 8. Ciprofloxacin-loading and release from PEG/PAE-DNase micelles. (a) Drug loading content (DLC) of ciprofloxacin in PEG/PAE-DNase and PEG/PAE micelles as a function of the feed ratio of ciprofloxacin to polymer (by weight). (b) Cumulative release of ciprofloxacin as a function of time for micelles self-assembly at a feed ratio of ciprofloxacin to polymer of 1:5 (ciprofloxacin loading at a concentration of 80 μg/mL) at pH 7.4 or 5.0 in PBS. Error bars denote SDs over three experiments with separately prepared micelle batches.

fact, lung tissue of mice treated with ciprofloxacin-loaded PEG/PAE-DNase micelles, resembled lung tissue of uninfected mice at sacrifice (Fig. 10g).

Histological examination of heart, liver, spleen and kidney tissues confirmed biosafety of ciprofloxacin-loaded PEG/PAE-DNase micelles by comparison of H&E stained tissues of uninfected mice (Fig. S10). Similarly, also hematological parameters were all within the same level compared for uninfected mice and mice treated with ciprofloxacin-loaded PEG/PAE-DNase micelles (Fig. S11).

4. Discussion

Biofilm dispersants, are considered promising for assisting antibiotic killing of bacteria through the degradation of the matrix of infectious biofilms [46]. eDNA plays a crucial role in keeping infectious biofilms together [13]. In order to prevent bacteria dispersed from a biofilm to cause infection elsewhere in the body [47]. dispersant action should be well synchronized with antibiotic killing. The clinical application of DNase as a dispersant of infectious biofilms has long been considered based on *in vitro* studies [18]. However, co-administration of DNase together with an antibiotic through injection in patients has remained impossible due to rapid, enzymatic inactivation of DNase in the blood

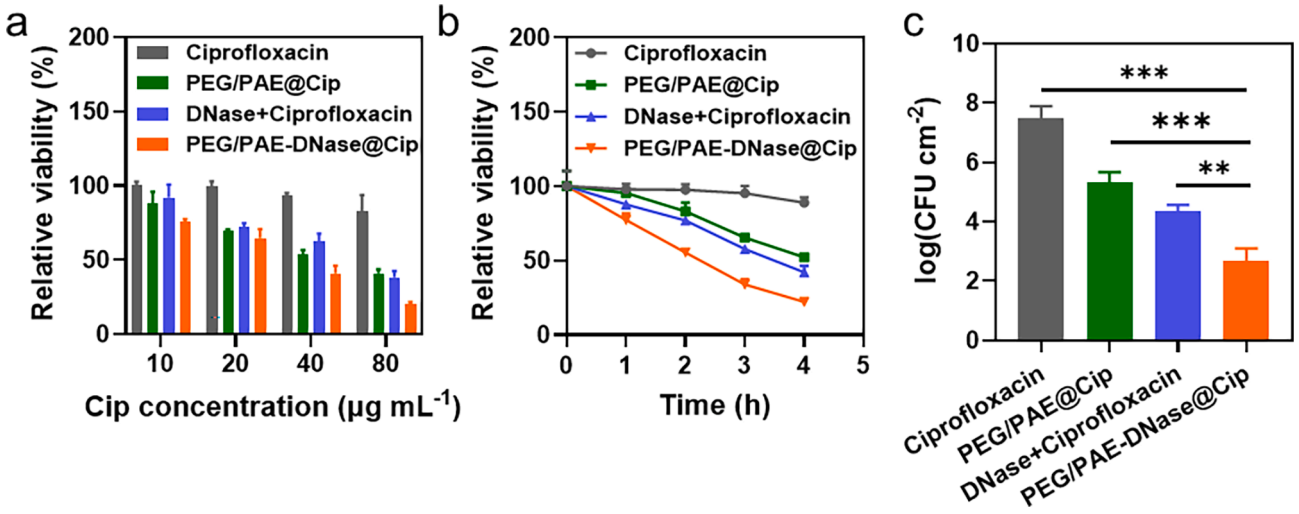

Fig. 9. *In vitro* eradication of a *S. aureus* ATCC12600^{GFP} biofilm by 4 h exposure to ciprofloxacin in solution in absence or presence of DNase or loaded in different micelles. (a) Viability of staphylococci after exposure to different ciprofloxacin equivalent concentrations. Staphylococcal viability was assessed from the green fluorescence of *S. aureus* ATCC12600^{GFP} biofilms, setting green fluorescence of biofilms after exposure to TSB at 100 %. (b) Viability of staphylococci as a function of time after exposure to ciprofloxacin at a ciprofloxacin equivalent concentration of 80 μg/mL. Green fluorescence of *S. aureus* ATCC12600^{GFP} biofilms prior to ciprofloxacin exposure was set to 100 %. (c) Number of *S. aureus* CFUs after exposure to ciprofloxacin at a ciprofloxacin equivalent concentration of 80 μg/mL. Error bars denote SDs over three experiments with separately prepared micelle batches and differently grown staphylococcal cultures. ** and *** indicate statistically significant differences at $P < 0.01$ and $P < 0.001$, respectively (one way ANOVA).

circulation [26]. In this paper, we designed a pH-responsive micellar nanocarrier, with DNase conjugated to PAE inside the micellar shell, and core-loaded with ciprofloxacin. In-shell protection of DNase prevented enzymatic inactivation during blood circulation at physiological pH, while in the acidic environment of an infectious biofilm, DNase was exposed and degraded the biofilm. At the same time, core-loaded ciprofloxacin was released and killed the dispersed bacteria and remaining biofilm.

Although DNase has been applied in the clinic for decades particularly to improve lung function in cystic fibrosis patients through cleavage of DNA in sputum [48]. the short, terminal half-life of DNase in blood prevents DNase injection for the treatment of infectious biofilms [28]. Previously, DNase coated nanoparticles were reported to maintain a higher concentration of DNase *in vivo* compared with free DNase in solution [49–51], but this approach still exposes DNase to blood-borne enzymes when injected. Moreover, this approach does not include the self-targeting ability facilitated by our PEG/PAE-DNase micelles. Stealth circulation of PEG/PAE-DNase micelles was ensured for well over 24 h due to the PEG component in the micellar shell, while the PAE component enabled self-targeting from a mouse tail towards a biofilm in the lung of a mouse within 4 h, as a result of charge reversal upon a decrease in pH from 7.4 in blood to below 6.5 in a biofilm [52]. Once inside a biofilm, dispersal by DNase and ciprofloxacin killing yielded better bacterial killing than could be achieved by ciprofloxacin alone, ciprofloxacin co-administered with DNase in solution or loaded in PEG/PAE micelles without DNase conjugated to the PAE block.

Nosocomial infection has a high mortality rate [33]. as reflected in our current study design in which all mice suffering from staphylococcal pneumonia died without treatment, while all mice in the group treated with PEG/PAE-DNase micelles and core-loaded with ciprofloxacin survived. Since survival is the ultimate goal of clinical treatment [53], this arguably constitutes the strongest point in favor of advocating the further exploration and clinical translation of PEG/PAE-DNase micelles and core-loaded with an antibiotic. Since clinically dispersed bacteria are not only killed more easily by antibiotics, but are also more prone to clearance from the blood by immune cells [54], PEG/PAE-DNase micelles may also be effective against antibiotic-resistant bacteria. As a final point in favor of further exploration and clinical translation of PEG/PAE-DNase micelles and core-loaded with antibiotics, other studies have shown that PEG/PAE micelles with PAE conjugated DNase, were able to find their way after tail-vein injection towards an abdominal biofilm [29] as well as to subcutaneous biofilms [52,55].

Development of new antibiotics requires a long period times and huge expenses while the time between clinical introduction and the discovery of the first resistant bacterial strains becomes ever shorter [56]. Strategies to make better use of existing antibiotics is a more feasible approach in the clinical treatment of biofilm infections [57] to which end PEG/PAE-DNase micelles may contribute.

5. Conclusion

In conclusion, PEG/PAE-DNase micelles with DNase conjugated to PAE-blocks inside the micellar shell and core-loaded with ciprofloxacin have been successfully synthesized. At physiological pH, this conjugation protected DNase inside the micellar shell against inactivation by blood-borne enzymes. Upon injection in the blood circulation, these micelles self-targeted to an infectious biofilm, while PAE becomes positively charged and hydrophilic. This yielded accumulation in biofilms and stretched the PAE to expose DNase and release of ciprofloxacin. Accordingly, DNase dispersed the biofilm and the simultaneous release of ciprofloxacin ensured killing of dispersed bacteria. Pneumonia in a mouse model could be more effectively treated with our newly designed micelles than by ciprofloxacin co-administered with or without DNase in solution, or PEG/PAE micelles core-loaded with ciprofloxacin but without PAE-conjugated DNase. Micelles were fully biosafe with affecting major organ tissues or blood parameters.

Considering that DNase is clinically approved for use in cystic fibrosis patients, this paves the way for clinical translation of ciprofloxacin-loaded, PEG/PAE-DNase micelles for the treatment of pneumonia and other infections that can be reached through self-targeting after blood-injection.

Declaration of Competing Interest

H.J.B. is director-owner of a consulting company, SASA BV. The authors declare that they have no known competing financial interests or personal relationships that could have appeared to influence the work reported in this paper.

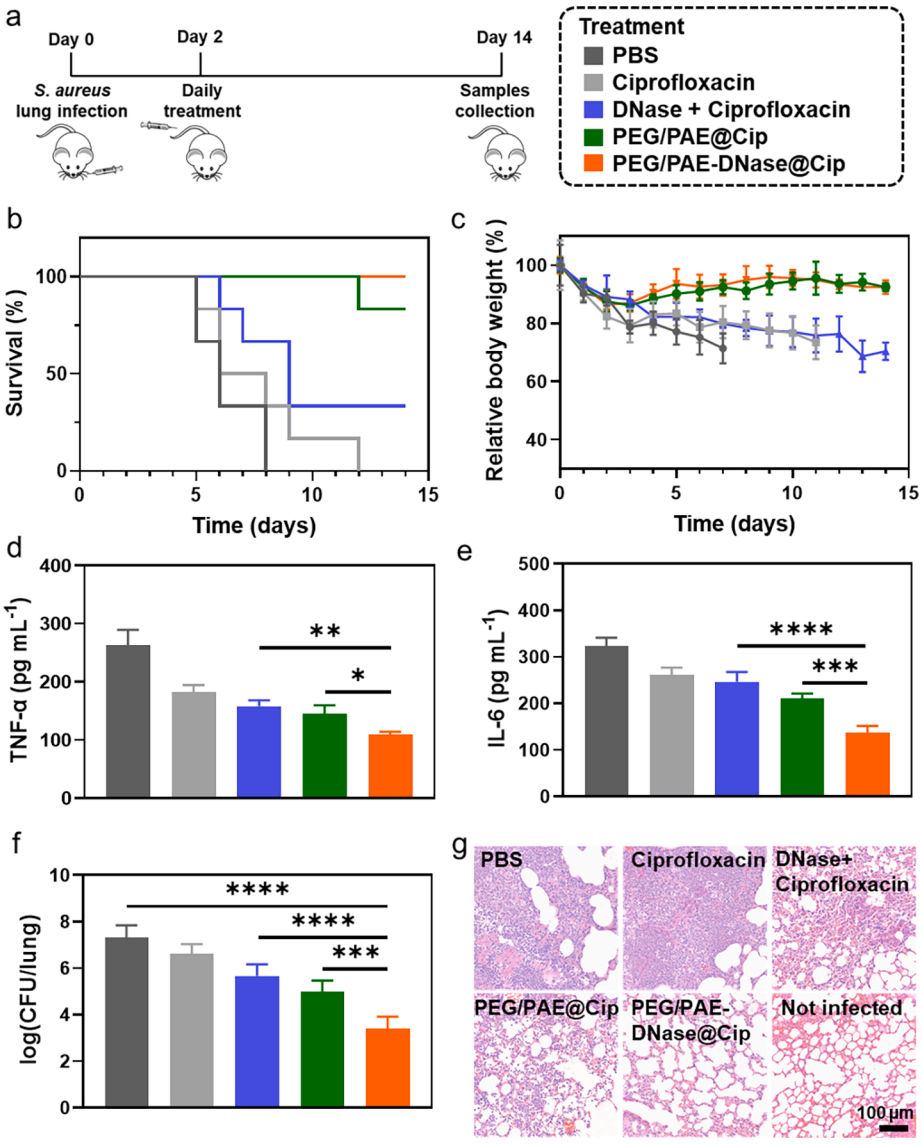

Fig. 10. *In vivo* eradication of a *S. aureus*ATCC12600^{GFP} biofilm in a murine pneumonia model by ciprofloxacin-loaded PEG/PAE-DNase micelles. (a) Experimental scheme for staphylococcal pneumonia infection and treatment in mice (see also Fig. S7). Treatment consisted of daily tail-vein injections of PBS, ciprofloxacin in solution in absence or presence of DNase and ciprofloxacin loaded in micelles (ciprofloxacin dose 10 mg/kg body weight). Each group consists of six mice. (b) Kaplan-Meier survival curve of mice as a function of time. (c) Body weight of mice, expressed as a percentage weight of the weight at entry in the study, set at 100 %. Error bars denote SDs over the surviving mice in each group. (d) TNF-α within the lungs of mice. (e) IL-6 within the lungs of mice. (f) Number of *S. aureus* CFUs isolated from the lungs of mice after sacrifice. Error bars denote SDs over three mice. *, **, *** and **** indicates statistically significant differences at $P < 0.05$, $P < 0.01$, $P < 0.001$ and $P < 0.0001$ (one way ANOVA), respectively. (g) Hematoxylin and eosin (H&E)-stained tissue sections from mice at sacrifice. Magnification used is 20 ×.

Data availability

Data will be made available on request.

Acknowledgments

This work was financial supported by the National Natural Science Foundation of China (No. 51933006).

Appendix A. Supplementary data

Supplementary data to this article can be found online at https://doi.org/10.1016/j.cej.2022.139619.

References

[1] M. Okshevsky, V.R. Regina, R.L. Meyer, Extracellular DNA as a target for biofilm control, Curr. Opin. Biotechnol. 33 (2015) 73–80, https://doi.org/10.1016/j.copbio.2014.12.002.
[2] W.-J. Chen, T.-H. Liao, Structure and function of bovine pancreatic deoxyribonuclease I, Protein Pept. Lett. 13 (2006) 447–453, https://doi.org/10.2174/092986606776819475.
[3] M. Okshevsky, R.L. Meyer, The role of extracellular DNA in the establishment, maintenance and perpetuation of bacterial biofilms, Crit. Rev. Microbiol. 41 (2015) 341–352, https://doi.org/10.3109/1040841X.2013.841639.
[4] O. Zafra, M. Lamprecht-Grandío, C.G. de Figueras, J.E. González-Pastor, T. Msadek, Extracellular DNA release by undomesticated Bacillus subtilis is regulated by early competence, PLoS ONE. 7 (11) (2012) e48716.
[5] A.L. Ibanez de Aldecoa, O. Zafra, J.E. Gonzalez-Pastor, Mechanisms and regulation of extracellular DNA release and its biological roles in microbial communities, Front. Microbiol. 8 (2017) 1390, https://doi.org/10.3389/fmicb.2017.01390.
[6] R. Biswas, L. Voggu, U.K. Simon, P. Hentschel, G. Thumm, F. Gotz, Activity of the major staphylococcal autolysin Atl, FEMS Microbiol. Lett. 259 (2006) 260–268, https://doi.org/10.1111/j.1574-6968.2006.00281.x.
[7] L. Turnbull, M. Toyofuku, A.L. Hynen, M. Kurosawa, G. Pessi, N.K. Petty, S. R. Osvath, G. Carcamo-Oyarce, E.S. Gloag, R. Shimoni, U. Omasits, S. Ito, X. Yap, L. G. Monahan, R. Cavaliere, C.H. Ahrens, I.G. Charles, N. Nomura, L. Eberl, C. B. Whitchurch, Explosive cell lysis as a mechanism for the biogenesis of bacterial membrane vesicles and biofilms, Nat. Commun. 7 (2016) 11220, https://doi.org/10.1038/ncomms11220.
[8] A.P. Roberts, J. Pratten, M. Wilson, P. Mullany, Transfer of a conjugative transposon, Tn5397 in a model oral biofilm, FEMS Microbiol. Lett. 177 (1999) 63–66, https://doi.org/10.1111/j.1574-6968.1999.tb13714.x.
[9] K. Abe, N. Nomura, S. Suzuki, Biofilms: hot spots of horizontal gene transfer (HGT) in aquatic environments, with a focus on a new HGT mechanism, FEMS Microbiol. Ecol. 96 (2020) fiaa031, https://doi.org/10.1093/femsec/fiaa031.
[10] H. Mulcahy, L. Charron-Mazenod, S. Lewenza, M.S. Gilmore, Extracellular DNA chelates cations and induces antibiotic resistance in Pseudomonas aeruginosa biofilms, PLoS Pathog. 4 (11) (2008) e1000213.
[11] M. Wilton, L. Charron-Mazenod, R. Moore, S. Lewenza, Extracellular DNA acidifies biofilms and induces aminoglycoside resistance in Pseudomonas aeruginosa, Antimicrob. Agents Chemother. 60 (2016) 544–553, https://doi.org/10.1128/AAC.01650-15.

[12] T. Das, P.K. Sharma, H.J. Busscher, H.C. van der Mei, B.P. Krom, Role of extracellular dna in initial bacterial adhesion and surface aggregation, Appl. Environ. Microbiol. 76 (2010) 3405–3408, https://doi.org/10.1128/AEM.03119-09.

[13] T. Das, S. Sehar, M. Manefield, The roles of extracellular DNA in the structural integrity of extracellular polymeric substance and bacterial biofilm development, Env. Microbiol Rep. 5 (2013) 778–786, https://doi.org/10.1111/1758-2229.12085.

[14] C.B. Whitchurch, T. Tolker-Nielsen, P.C. Ragas, J.S. Mattick, Extracellular DNA required for bacterial biofilm formation, Science. 295 (2002) 1487–1487. https://doi.org/10.1126/science.295.5559.1487.

[15] J.T. Blakeman, A.L. Morales-García, J. Mukherjee, K. Gori, A.S. Hayward, N. J. Lant, M. Geoghegan, Extracellular DNA provides structural integrity to a Micrococcus luteus biofilm, Langmuir. 35 (2019) 6468–6475, https://doi.org/10.1021/acs.langmuir.9b00297.

[16] T. Das, B.P. Krom, H.C. van der Mei, H.J. Busscher, P.K. Sharma, DNA-mediated bacterial aggregation is dictated by acid–base interactions, Soft Matter. 7 (2011) 2927–2935, https://doi.org/10.1039/C0SM01142H.

[17] J.J.T.M. Swartjes, T. Das, S. Sharifi, G. Subbiahdoss, P.K. Sharma, B.P. Krom, H. J. Busscher, H.C. van der Mei, A functional DNase I coating to prevent adhesion of bacteria and the formation of biofilm, Adv. Funct. Mater. 23 (2013) 2843–2849, https://doi.org/10.1002/adfm.201202927.

[18] S. Wongkaewkhiaw, S. Kanthawong, J.G.M. Bolscher, K. Nazmi, S. Taweechaisupapong, B.P. Krom, DNase-mediated eDNA removal enhances D-LL-31 activity against biofilms of bacteria isolated from chronic rhinosinusitis patients, Biofouling. 36 (2020) 1117–1128, https://doi.org/10.1080/08927014.2020.1857741.

[19] C. Liu, Y. Zhao, W. Su, J. Chai, L. Xu, J. Cao, Y. Liu, Encapsulated DNase improving the killing efficiency of antibiotics in staphylococcal biofilms, J. Mater. Chem. B. 8 (2020) 4395–4401, https://doi.org/10.1039/D0TB00441C.

[20] W. Tasia, C. Lei, Y. Cao, Q. Ye, Y. He, C. Xu, Enhanced eradication of bacterial biofilms with DNase I-loaded silver-doped mesoporous silica nanoparticles, Nanoscale. 12 (2020) 2328–2332, https://doi.org/10.1039/C9NR08467C.

[21] S.R. Hymes, T.M. Randis, T.Y. Sun, A.J. Ratner, DNase inhibits Gardnerella vaginalis biofilms in vitro and in vivo, J. Infect. Dis. 207 (2013) 1491–1497, https://doi.org/10.1093/infdis/jit047.

[22] J.B. Kaplan, K. LoVetri, S.T. Cardona, S. Madhyastha, I. Sadovskaya, S. Jabbouri, E. A. Izano, Recombinant human DNase I decreases biofilm and increases antimicrobial susceptibility in staphylococci, J. Antibiot. (Tokyo) 65 (2012) 73–77, https://doi.org/10.1038/ja.2011.113.

[23] M. Kovaliov, D. Cohen-Karni, K.A. Burridge, D. Mambelli, S. Sloane, N. Daman, C. Xu, J. Guth, J. Kenneth Wickiser, N. Tomycz, R.C. Page, D. Konkolewicz, S. Averick, Grafting strategies for the synthesis of active DNase I polymer biohybrids, Eur. Polym. J. 107 (2018) 15–24, https://doi.org/10.1016/j.eurpolymj.2018.07.041.

[24] R. Lichtinghagen, Determination of Pulmozyme®(dornase alpha) stability using a kinetic colorimetric DNase I activity assay, Eur. J. Pharm. Biopharm. 63 (2006) 365–368, https://doi.org/10.1016/j.ejpb.2006.03.001.

[25] S.S. Abdel-Gany, M.O. El-Badry, A.S. Fahmy, S.A. Mohamed, Purification and characterization of deoxyribonuclease from small intestine of camel Camelus dromedarius, J. Genet. Eng. Biotechnol. 15 (2017) 463–467, https://doi.org/10.1016/j.jgeb.2017.06.008.

[26] W.S. Prince, D.L. Baker, A.H. Dodge, A.E. Ahmed, R.W. Chestnut, D.V. Sinicropi, Pharmacodynamics of recombinant human DNase I in serum, Clin. Exp. Immunol. 113 (2001) 289–296, https://doi.org/10.1046/j.1365-2249.1998.00647.x.

[27] Y.Y. Lee, H.H. Park, W. Park, H. Kim, J.G. Jang, K.S. Hong, J.-Y. Lee, H.S. Seo, D. H. Na, T.-H. Kim, Y.B. Choy, J.H. Ahn, W. Lee, C.G. Park, Long-acting nanoparticulate DNase-1 for effective suppression of SARS-CoV-2-mediated neutrophil activities and cytokine storm, Biomaterials. 267 (2021), 120389, https://doi.org/10.1016/j.biomaterials.2020.120389.

[28] M. Macanovic, D. Sinicropi, S. Shak, S. Baughman, S. Thiru, P.J. Lachmann, The treatment of systemic lupus erythematosus (SLE) in NZB/W F1 hybrid mice; studies with recombinant murine DNase and with dexamethasone, Clin. Exp. Immunol. 106 (1996) 243–252, https://doi.org/10.1046/j.1365-2249.1996.d01-839.x.

[29] S. Tian, L. Su, Y. Liu, J. Cao, G. Yang, Y. Ren, F. Huang, J. Liu, Y. An, H.C. van der Mei, H.J. Busscher, L. Shi, Self-targeting, zwitterionic micellar dispersants enhance antibiotic killing of infectious biofilms—An intravital imaging study in mice, Sci. Adv. 6 (2020) eabb1112, https://doi.org/10.1126/sciadv.abb1112.

[30] D. Wang, G. Yang, H.C. Mei, Y. Ren, H.J. Busscher, L. Shi, Liposomes with water as a ph-responsive functionality for targeting of acidic tumor and infection sites, Angew. Chem. Int. Ed. 60 (2021) 17714–17719, https://doi.org/10.1002/anie.202106329.

[31] S.E. Birk, A. Boisen, L.H. Nielsen, Polymeric nano-and microparticulate drug delivery systems for treatment of biofilms, Adv. Drug Deliv. Rev. 174 (2021) 30–52, https://doi.org/10.1016/j.addr.2021.04.005.

[32] A.W. Smith, Biofilms and antibiotic therapy: is there a role for combating bacterial resistance by the use of novel drug delivery systems? Adv. Drug Deliv. Rev. 57 (2005) 1539–1550, https://doi.org/10.1016/j.addr.2005.04.007.

[33] J.-L. Vincent, Nosocomial infections in adult intensive-care units, Lancet 361 (2003) 2068–2077, https://doi.org/10.1016/s0140-6736(03)13644-6.

[34] Y. Liu, H.J. Busscher, B. Zhao, Y. Li, Z. Zhang, H.C. van der Mei, Y. Ren, L. Shi, Surface-adaptive, antimicrobially loaded, micellar nanocarriers with enhanced penetration and killing efficiency in staphylococcal biofilms, ACS Nano. 10 (2016) 4779–4789, https://doi.org/10.1021/acsnano.6b01370.

[35] H. Ou, T. Cheng, Y. Zhang, J. Liu, Y. Ding, J. Zhen, W. Shen, Y. Xu, W. Yang, P. Niu, J. Liu, Y. An, Y. Liu, L. Shi, Surface-adaptive zwitterionic nanoparticles for prolonged blood circulation time and enhanced cellular uptake in tumor cells, Acta Biomater. 65 (2018) 339–348, https://doi.org/10.1016/j.actbio.2017.10.034.

[36] J. Li, H.J. Busscher, H.C. van der Mei, J. Sjollema, Surface enhanced bacterial fluorescence and enumeration of bacterial adhesion, Biofouling. 29 (2013) 11–19, https://doi.org/10.1080/08927014.2012.742074.

[37] Bacteria Collection: NCTC 8532 Staphylococcus aureus, Bact. Collect. NCTC 8532 Staphylococcus Aureus. (2022). https://www.culturecollections.org.uk/products/bacteria/detail.jsp?refId=NCTC+8532&collection=nctc (accessed May 3, 2022).

[38] Tech data sheet for Xen36 Staphylococcus aureus, Tech Data Sheet Xen36 Staphylococcus Aureus. (2022). https://resources.perkinelmer.com/lab-solutions/resources/docs/DTS_XenoLight_Xen36_119243.pdf (accessed May 3, 2022).

[39] R. Grande, M.C. Di Marcantonio, I. Robuffo, A. Pompilio, C. Celia, L. Di Marzio, D. Paolino, M. Codagnone, R. Muraro, P. Stoodley, L. Hall-Stoodley, G. Mincione, Helicobacter pylori ATCC 43629/NCTC 11639 outer membrane vesicles (OMVs) from biofilm and planktonic phase associated with extracellular DNA (eDNA), Front. Microbiol. 6 (2015) 1369, https://doi.org/10.3389/fmicb.2015.01369.

[40] A.I. Hidron, C.E. Low, E.G. Honig, H.M. Blumberg, Emergence of community-acquired meticillin-resistant Staphylococcus aureus strain USA300 as a cause of necrotising community-onset pneumonia, Lancet Infect. Dis. 9 (2009) 384–392, https://doi.org/10.1016/S1473-3099(09)70133-1.

[41] B. Manicassamy, S. Manicassamy, A. Belicha-Villanueva, G. Pisanelli, B. Pulendran, A. Garcia-Sastre, Analysis of in vivo dynamics of influenza virus infection in mice using a GFP reporter virus, Proc. Natl. Acad. Sci. 107 (2010) 11531–11536, https://doi.org/10.1073/pnas.0914994107.

[42] J.B. Wardenburg, R.J. Patel, O. Schneewind, Surface proteins and exotoxins are required for the pathogenesis of *Staphylococcus aureus* pneumonia, Infect. Immun. 75 (2007) 1040–1044, https://doi.org/10.1128/IAI.01313-06.

[43] R.H. Tullis, K.A. Dill, P.A. Price, Fluorescence and kinetic studies on the divalent metal ion induced conformational changes in DNase a, J. Biol. Chem. 256 (1981) 5656–5661, https://doi.org/10.1016/S0021-9258(19)69255-0.

[44] T. Cheng, R. Ma, Y. Zhang, Y. Ding, J. Liu, H. Ou, Y. An, J. Liu, L. Shi, A surface-adaptive nanocarrier to prolong circulation time and enhance cellular uptake, Chem. Commun. 51 (2015) 14985–14988, https://doi.org/10.1039/C5CC05854F.

[45] J. Barbosa, D. Barrón, E. Jiménez-Lozano, V. Sanz-Nebot, Comparison between capillary electrophoresis, liquid chromatography, potentiometric and spectrophotometric techniques for evaluation of pKa values of zwitterionic drugs in acetonitrile–water mixtures, Anal. Chim. Acta. 437 (2001) 309–321, https://doi.org/10.1016/S0003-2670(01)00997-7.

[46] S. Tian, H.C. van der Mei, Y. Ren, H.J. Busscher, L. Shi, Recent advances and future challenges in the use of nanoparticles for the dispersal of infectious biofilms, J. Mater. Sci. Technol. 84 (2021) 208–218, https://doi.org/10.1016/j.jmst.2021.02.007.

[47] D. Fleming, K. Rumbaugh, The consequences of biofilm dispersal on the host, Sci. Rep. 8 (2018) 10738, https://doi.org/10.1038/s41598-018-29121-2.

[48] R. Suri, The use of human deoxyribonuclease (rhDNase) in the management of cystic fibrosis, BioDrugs. 19 (2005) 135–144, https://doi.org/10.2165/00063030-200519030-00001.

[49] A. Baelo, R. Levato, E. Julián, A. Crespo, J. Astola, J. Gavaldà, E. Engel, M. A. Mateos-Timoneda, E. Torrents, Disassembling bacterial extracellular matrix with DNase-coated nanoparticles to enhance antibiotic delivery in biofilm infections, J. Controlled Release. 209 (2015) 150–158, https://doi.org/10.1016/j.jconrel.2015.04.028.

[50] Y. Xie, W. Zheng, X. Jiang, Near-infrared light-activated phototherapy by gold nanoclusters for dispersing biofilms, ACS Appl. Mater. Interfaces. 12 (2020) 9041–9049, https://doi.org/10.1021/acsami.9b21777.

[51] Y. Tan, S. Ma, M. Leonhard, D. Moser, G.M. Haselmann, J. Wang, D. Eder, B. Schneider-Stickler, Enhancing antibiofilm activity with functional chitosan nanoparticles targeting biofilm cells and biofilm matrix, Carbohydr. Polym. 200 (2018) 35–42, https://doi.org/10.1016/j.carbpol.2018.07.072.

[52] Y. Liu, H.C. van der Mei, B. Zhao, Y. Zhai, T. Cheng, Y. Li, Z. Zhang, H.J. Busscher, Y. Ren, L. Shi, Eradication of multidrug-resistant *Staphylococcal* infections by light-activatable micellar nanocarriers in a murine model, Adv. Funct. Mater. 27 (2017) 1701974, https://doi.org/10.1002/adfm.201701974.

[53] H.J. Busscher, W. Woudstra, T.G. van Kooten, P. Jutte, L. Shi, J. Liu, W.L. J. Hinrichs, H.W. Frijlink, R. Shi, J. Liu, J. Parvizi, S. Kates, V.M. Rotello, T. P. Schaer, D. Williams, D.W. Grainger, H.C. van der Mei, Accepting higher morbidity in exchange for sacrificing fewer animals in studies developing novel infection-control strategies, Biomaterials. 232 (2020), 119737, https://doi.org/10.1016/j.biomaterials.2019.119737.

[54] K.P. Rumbaugh, K. Sauer, Biofilm dispersion, Nat. Rev. Microbiol. 18 (2020) 571–586, https://doi.org/10.1038/s41579-020-0385-0.

[55] S. Hussain, J. Joo, J. Kang, B. Kim, G.B. Braun, Z.-G. She, D. Kim, A.P. Mann, T. Mölder, T. Teesalu, S. Carnazza, S. Guglielmino, M.J. Sailor, E. Ruoslahti, Antibiotic-loaded nanoparticles targeted to the site of infection enhance antibacterial efficacy, Nat. Biomed. Eng. 2 (2018) 95–103, https://doi.org/10.1038/s41551-017-0187-5.

[56] L.J. Piddock, The crisis of no new antibiotics—what is the way forward? Lancet Infect. Dis. 12 (2012) 249–253, https://doi.org/10.1016/S1473-3099(11)70316-4.

[57] G.D. Wright, Antibiotic adjuvants: rescuing antibiotics from resistance, Trends Microbiol. 24 (2016) 862–871, https://doi.org/10.1016/j.tim.2016.06.009.